Science and Technology Indonesia
e-ISSN:2580-4391 p-ISSN:2580-4405
Vol. 11, No. 1, January 2026

Research Paper

Electrochemically Deposited rGO–Cu_2S Composite as a High-Performance Counter Electrode for Quantum Dot-Sensitized Solar Cells

Nguyen Thuy Kieu Duyen[1], Nguyen Thi My Hanh[2,3,4*], Le Van Hieu[3,5], Thi Viet Ha Luu[1], Huu Phuc Dang[6]

[1]*Faculty of Chemical Engineering, Industrial University of Ho Chi Minh City, Ho Chi Minh City, 700000, Vietnam*
[2]*Faculty of Physics & Engineering Physics, VNUHCM-University of Science, Ho Chi Minh City, 700000, Vietnam*
[3]*Vietnam National University Ho Chi Minh City, Ho Chi Minh City, 700000, Vietnam*
[4]*Faculty of Mechanical Engineering, Industrial University of Ho Chi Minh City, Ho Chi Minh City, 700000, Vietnam*
[5]*Faculty of Materials Science and Technology, University of Science, VNU–HCMC, Ho Chi Minh City, 700000, Vietnam*
[6]*Faculty of Fundamental Science, Industrial University of Ho Chi Minh City, Ho Chi Minh City, 700000, Vietnam*
*__Corresponding author__: nguyenthimyhanh@iuh.edu.vn

Abstract

This study reports the development of reduced graphene oxide (rGO), copper sulfide (Cu_2S), and their hybrid composite (rGO-Cu_2S) as counter electrodes (CEs) for quantum dot-sensitized solar cells (QDSSCs). The electrodes were fabricated on FTO substrates via a simple, low-temperature electrochemical deposition method. Morphological analysis revealed flower-like Cu_2S nanostructures and wrinkled rGO sheets, while the composite combined these features into a uniform hybrid layer. Electrochemical measurements demonstrated that the rGO-Cu_2S CE exhibited superior catalytic activity and lower charge-transfer resistance compared to the individual materials. When integrated into QDSSCs, the rGO-Cu_2S electrode achieved the highest power conversion efficiency (4.65%), outperforming Cu_2S (3.77%) and rGO (3.24%). The synergistic interaction between conductive rGO networks and catalytically active Cu_2S nanostructures underpin this improvement, highlighting rGO-Cu_2S as a cost-effective and efficient alternative to noble-metal-based counter electrodes.

Keywords

Quantum Dot-Sensitized Solar Cells (QDSSCs), Electrochemical Deposition, Hybrid Nanocomposite, rGO-Cu_2S, Counter Electrode

Received: 11 July 2025, Accepted: 6 September 2025
https://doi.org/10.26554/sti.2026.11.1.1-9

1. INTRODUCTION

The evolution of photovoltaic technologies has given rise to third-generation solar cells, which aim to overcome the cost and efficiency limitations inherent to traditional silicon-based (first generation) and thin-film (second generation) devices. These advanced concepts-encompassing dye-sensitized solar cells (DSSCs), perovskite solar cells (PSCs), and quantum dot-sensitized solar cells (QDSSCs)-capitalize on novel photoactive materials and low-temperature processing routes, thereby offering the prospect of high power conversion efficiency (PCE) at reduced manufacturing cost (Kusumawati et al., 2024; Telussa et al., 2022). Among them, QDSSCs have attracted considerable attention due to the advantageous properties of quantum dots, such as tunable band gaps, large absorption coefficients, and facile solution processing (Chung et al., 2021; Nozik, 2002). A key component in QDSSCs is the counter electrode (CE), which is responsible for catalyzing the redox reaction of the electrolyte and regenerating the oxidized species (Du et al., 2016; Van Le et al., 2017). Traditionally, platinum has been widely used as the CE material (Meng et al., 2015), due to its superior electrocatalytic activity; however, its high cost, scarcity, and poor stability in polysulfide-based electrolytes limit its practical applications (Mehmood and Ul Haq Khan, 2019). Consequently, significant attention has shifted to earth-abundant alternatives such as copper sulfide (Cu_2S) (Jo et al., 2020; Wang et al., 2018; Ye et al., 2014) and carbon-based materials like reduced graphene oxide (rGO) (López-Rojas et al., 2024; Monika et al., 2022; Rathnavel et al., 2023). Copper sulfide (Cu_2S) exhibits excellent catalytic activity for polysulfide redox couples owing to its favorable band structure and high affinity for sulfide ions. However, it suffers from intrinsic limitations, such as low electrical conductivity, poor adhesion to substrates, and structural degradation under long-term cycling conditions. To address these issues, various transition metal sulfides-including nickel sulfide (NiS), cobalt sulfide (CoSx) (Que et al., 2014; Yang et al., 2019), and molybdenum sulfide (MoS_2) (Eryiğit et al., 2022; Tian et al., 2020), have also been explored as alternative electrocatalysts in energy conversion

systems due to their multiple oxidation states and good electrochemical stability. Despite their potential, these sulfides often face challenges such as particle agglomeration, sluggish kinetics, and the need for high-temperature synthesis. Reduced graphene oxide (rGO), on the other hand, provides excellent electrical conductivity, large specific surface area, and chemical robustness, making it an ideal supporting matrix or co-catalyst. The incorporation of rGO into metal sulfide-based electrodes not only enhances charge transport pathways but also stabilizes the catalytic material, prevents agglomeration, and improves the mechanical integrity of the hybrid film (Radich et al., 2011). Combining Cu_2S with rGO into a hybrid rGO@Cu_2S composite allows for a synergistic enhancement in electron transfer and catalytic activity due to the complementary properties of both materials (My Hanh et al., 2024; Ye et al., 2014).

Recent investigations have validated this hybrid approach. Prasad et al. (2021) employed an electrochemical co-reduction method followed by sulfurization to synthesize rGO-Cu_2S CEs, achieving a PCE of 4.26%, outperforming pristine Cu_2S (3.77%) and Pt (2.44%). The improved performance was attributed to reduced charge-transfer resistance (Rct), increased electrochemically active surface area, and enhanced electron transport across the electrode- electrolyte interface. Likewise, Malavekar et al. (2020) fabricated rGO-CuS hybrid layers via successive ionic layer adsorption and reaction (SILAR), obtaining improved conductivity, larger active surface area, and lower resistance in supercapacitor devices. Although their work was not directly applied to QDSSCs, it underlines the advantages of layered rGO-CuS architectures for electrochemical applications (Krishna Prasad et al., 2021).

In the present work, we describe the preparation of rGO, Cu_2S, and rGO@Cu_2S counter electrodes by electrochemical deposition. This approach was chosen for its simplicity, controllability, and compatibility with scalable and flexible device fabrication. Unlike conventional annealing or solvothermal synthesis, electrodeposition enables direct film growth on FTO substrates at ambient conditions, ensuring good adhesion and tunable morphology. Both sequential and co-deposition strategies can be employed, offering the opportunity to fabricate uniform hybrid films with optimized interfacial properties.

2. EXPERIMENTAL SECTION

2.1 Materials

Commercially available graphene oxide dispersion (4 mg/mL in water) was used as the precursor for reduced graphene oxide (rGO). Copper(II) nitrate trihydrate ($Cu(NO_3)_2{\cdot}3H_2O$, analytical grade, Sigma-Aldrich) was used as the Cu^{2+} source for the electrodeposition of copper sulfide. Thiourea (CH_4N_2S), analytical grade, Sigma-Aldrich) was used as the sulfur precursor for the formation of Cu_2S. Ethanol, acetone, and deionized (DI) water were used to clean the FTO substrates. Fluorine-doped tin oxide (FTO)-coated glass substrates (sheet resistance 15 ω/sq) were used as the conductive support for all electrodepositions.

2.2 Instruments

The structural and surface features of the prepared electrodes were examined using a series of standard characterization tools. Phase identification was conducted through X-ray diffraction (XRD, Bruker D8 Advance) employing Cu Kα radiation (λ = 1.5406 Å). The surface topography was observed by field-emission scanning electron microscopy (FESEM, Hitachi S-4800), while the associated elemental composition and spatial distribution were analyzed with an energy-dispersive X-ray spectroscopy (EDS) detector from Oxford Instruments integrated into the same system. Electrochemical behavior was evaluated by cyclic voltammetry (CV) and electrochemical impedance spectroscopy (EIS) using a CHI 650E workstation (CH Instruments, USA). Photovoltaic characterization of the QDSSCs was carried out through current–voltage (J–V) testing on a Keithley 2450 under simulated sunlight (AM 1.5G, 100 mW cm^{-2}) generated by a Newport Oriel xenon arc lamp equipped with an AM 1.5G filter.

2.3 Fabrication of Photoanode FTO/TiO_2/CdS/CdSe: Cu/ZnS

FTO/TiO_2/CdS/CdSe:Cu/ZnS photoanodes were prepared by combining screen printing and the SILAR technique. FTO glass substrates were ultrasonically cleaned with acetone, ethanol, and deionized water, followed by deposition of a TiO_2 film via screen printing, drying at 85°C for 45 min, and annealing at 500°C for 30 min. CdS and Cu^{2+}-doped CdSe QDs (Cd^{2+}/Cu^{2+} molar ratio = 0.3) were then deposited by SILAR using the reported precursor solutions (Dang et al., 2024). A ZnS passivation layer was subsequently introduced by SILAR with 0.2 M $Zn(NO_3)_2$ and 0.2 M Na_2S in ethanol. The resulting electrodes were rinsed with ethanol and stored under inert gas in the dark until use.

2.4 Fabrication of Photocathode FTO/ECu_2S, FTO/ErGO, FTO/ECu2S@rGO

Counter electrodes (CEs) for quantum dot-sensitized solar cells (QDSSCs) were fabricated by electrochemically depositing rGO, copper sulfide (Cu_2S), and a composite of rGO and (Cu_2S) (rGO@(Cu_2S)) onto fluorine-doped tin oxide (FTO) glass substrates. Before deposition, the FTO substrates were sequentially cleaned with detergent, deionized water, ethanol, and acetone under ultrasonication and dried in air to remove any impurities. For rGO deposition, a graphene oxide (GO) dispersion was electrochemically reduced in a three-electrode configuration using FTO as the working electrode, a platinum wire as the counter electrode, and Ag/AgCl as the reference electrode in an aqueous electrolyte. (Cu_2S) films were prepared by electrodeposition of Cu^{2+} ions from an aqueous solution containing copper nitrate ($Cu(NO_3)_2$) and boric acid, followed by a sulfurization step in sodium sulfide solution to form crystalline (Cu_2S). Reduced graphene oxide (rGO) films were obtained by electrochemical reduction of graphene oxide (GO) on FTO substrates in a suitable electrolyte. For the hybrid, rGO-(Cu_2S) electrodes were synthesized by two approaches: (i) sequential

deposition, in which rGO was first electrodeposited and subsequently coated with (Cu_2S) followed by sulfurization, and (ii) one-step co-deposition, where GO and Cu^{2+} precursors were co-electrodeposited and then sulfurized to yield a uniform rGO-(Cu_2S) composite. These electrodes were finally applied as counter electrodes in QDSSCs assembled with a CdS/CdSe-sensitized TiO_2 photoanode and a polysulfide electrolyte.

2.5 Assembly of QDSSCs

The photoanode and counter electrode were encapsulated in a Surlyn packing material and infused with a redox electrolyte comprising 1 M Na_2S, 1 M S, and 0.1 M KCl, yielding an active area of 1 cm^2 for the cell.

2.6 Characteristics and Measurements

All materials were characterized using the instruments described above. Device photovoltaic performance was tested under simulated AM 1.5G conditions with calibrated irradiance of 100 mW cm^{-2}.

3. RESULTS AND DISCUSSION

The crystalline structures of the electrodeposited samples-Cu_2S (ECu_2S), reduced graphene oxide (ErGO), and their composite (ErGO-Cu_2S) were characterized using X-ray diffraction (XRD) (Figure 1). The ECu_2S pattern displays distinct peaks corresponding to the crystalline planes of Cu_2S, confirming the successful deposition of this phase (Zhang et al., 2020). The ErGO sample exhibits a broad diffraction peak centered around 2θ = 26°, indexed to the (002) plane of reduced graphene oxide, indicative of the partial restoration of the graphitic structure following the electrochemical reduction of graphene oxide (Li et al., 2022; Van Thang et al., 2023). In the composite ErGO-Cu_2S sample, diffraction peaks corresponding to both Cu_2S and rGO were present, along with additional peaks originating from the underlying fluorine-doped tin oxide (FTO) substrate. The crystalline of the samples was further evaluated from the XRD patterns (Figure 1) by analyzing the full width at half maximum (FWHM) of the major diffraction peaks. The calculated crystallite sizes using the Scherrer equation were approximately 21.3 nm for ECu_2S, 19.6 nm for ErGO, and 22.5 nm for the ErGO@Cu_2S composite. The relatively small crystallite sizes confirm the nanocrystalline nature of all samples. In addition, the degree of crystallinity, estimated from the ratio of integrated crystalline peak areas to the total diffracted intensity, was found to be 67% for ECu_2S, 61% for ErGO, and 72% for ErGO@Cu_2S. The simultaneous observation of Cu_2S and rGO features in the composite confirmed the co-deposition and structural integration of both components.

Field-emission scanning electron microscopy (FESEM) was employed to investigate the surface morphologies of the electrochemically deposited Cu_2S (ECu_2S) and reduced graphene oxide (ErGO) films. The FESEM image of ECu_2S (Figure 2a) shows a surface with densely packed spherical clusters composed of radially aligned nanoneedles, forming a distinctive flower-like architecture with 0.6–1.0 μm in diameter. This

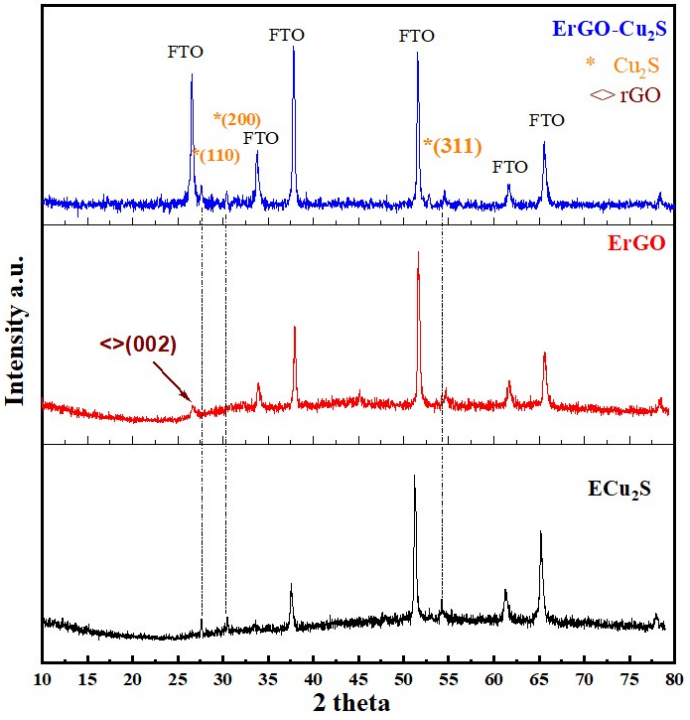

Figure 1. XRD Patterns of ErGO, ECu_2S, and ErGO@Cu_2S Films.

hierarchical structure offers a high surface area, which is advantageous for catalytic activity in counter electrode applications. In contrast, the ErGO film (Figure 2b) displayed a wrinkled and layered morphology typical of reduced graphene oxide, with partially overlapping sheets interspersed with nanoscale particles. This structure is indicative of the successful reduction of graphene oxide and provides a conductive and porous network that facilitates efficient charge transfer. The distinct morphological features of ECu_2S and ErGO (Figure 2c) suggest their potential for synergistic integration in hybrid rGO@Cu_2S counter electrodes to enhance the electrocatalytic performance of QDSSCs. To further analyze the morphology, the particle size distribution of the deposited nanostructures was evaluated from FESEM images using ImageJ software (Figures 2d, e, f). The histogram reveals that the average particle size of the ECu_2S sample is approximately 52 ± 12 nm, while the ErGO electrode shows slightly smaller and more uniform features with an average size of 38 ± 10 nm. In contrast, the ErGO@Cu_2S composite exhibits a broader distribution centered at 45 ± 15 nm, which can be attributed to the heterogeneous nucleation of Cu_2S nanoparticles on the rGO sheets. The narrower size distribution of ErGO compared to Cu_2S indicates that the rGO network acts as a template, restricting excessive growth and aggregation of Cu_2S domains.

The elemental distribution and composition of the ErGO@Cu_2S composite were analyzed using energy-dispersive X-ray spectroscopy (EDX), as shown in Figure 3. The EDX elemental mapping images confirmed the uniform and homogeneous

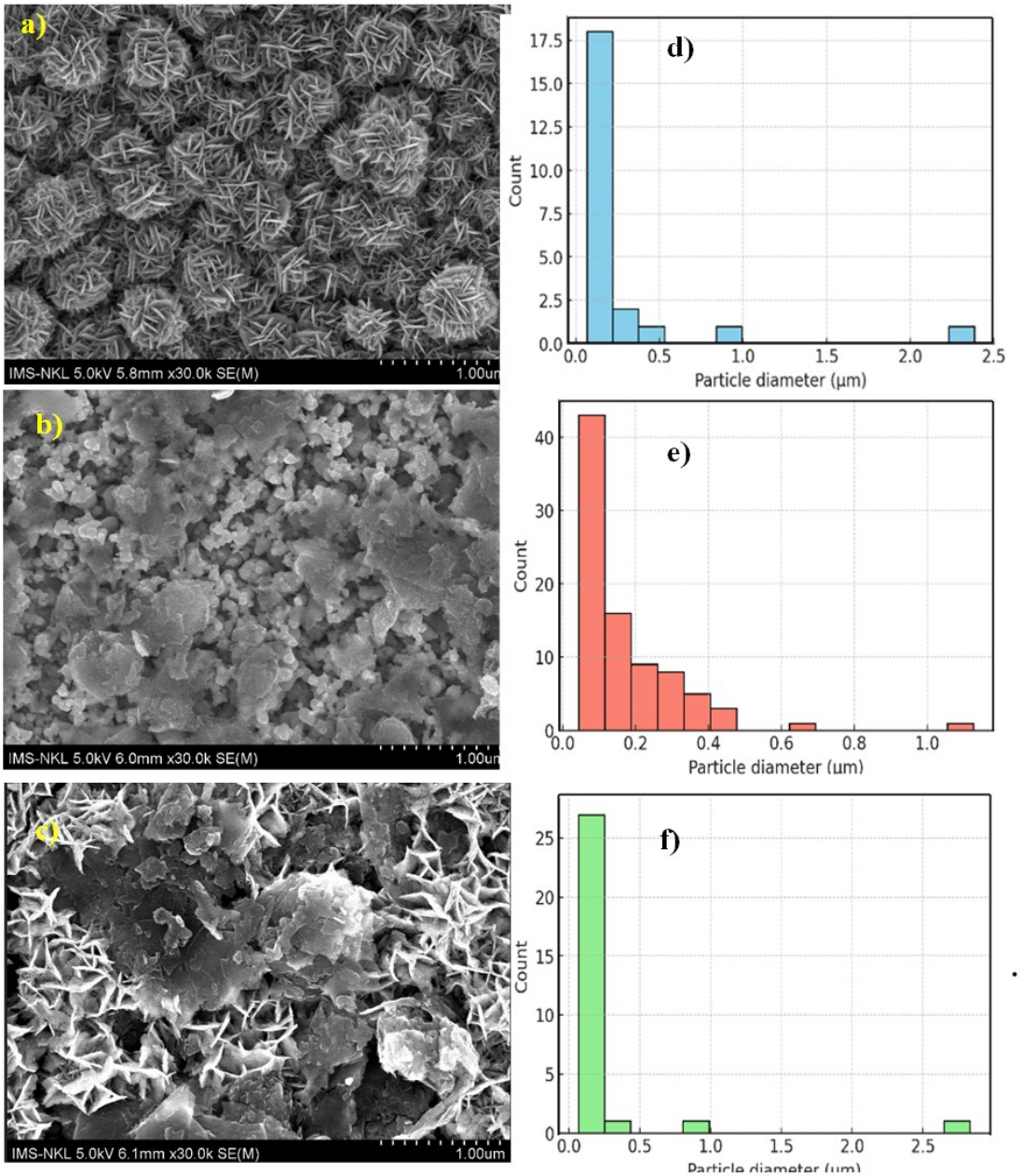

Figure 2. FESEM Images and Particle Size Distribution Histogram of a) d) ECu_2S, b) e) ErGO, and c), f) ErGO@Cu_2S Films

distribution of oxygen (O), carbon (C), copper (Cu), and sulfur (S) throughout the composite layer. Specifically, the presence of C and O (Figures 3a and 3b) is associated with the reduced graphene oxide (rGO) sheets, while the Cu and S signals (Figures 3c and 3d) confirm the successful electrodeposition of Cu_2S onto the rGO framework. The EDX spectrum and quantitative analysis (Figure 3k) further support the composite structure, with atomic percentages of C (26.45%), O (49.54%), Cu (17.94%), and S (6.06%). The relatively high oxygen and carbon content is consistent with partially reduced GO, indicating the presence of residual oxygen-containing functional groups. These groups may assist in anchoring the Cu_2S nanostructures and enhancing the interfacial contact. The Cu−to−S atomic ratio was approximately 3:1, suggesting the presence of excess copper species, possibly due to a Cu-rich phase or a slight deviation from stoichiometric Cu_2S, which is common in electrochemical deposition processes. For comparison, mapping of the individual components (ECu_2S and ErGO, Figures 3e, f, m and 3g, h, and l) also confirmed the homogeneous distribution of Cu/S and C/O, respectively, further supporting the reliability of the composite formation. Overall, the EDX results demonstrate that the ErGO@Cu_2S electrode contains

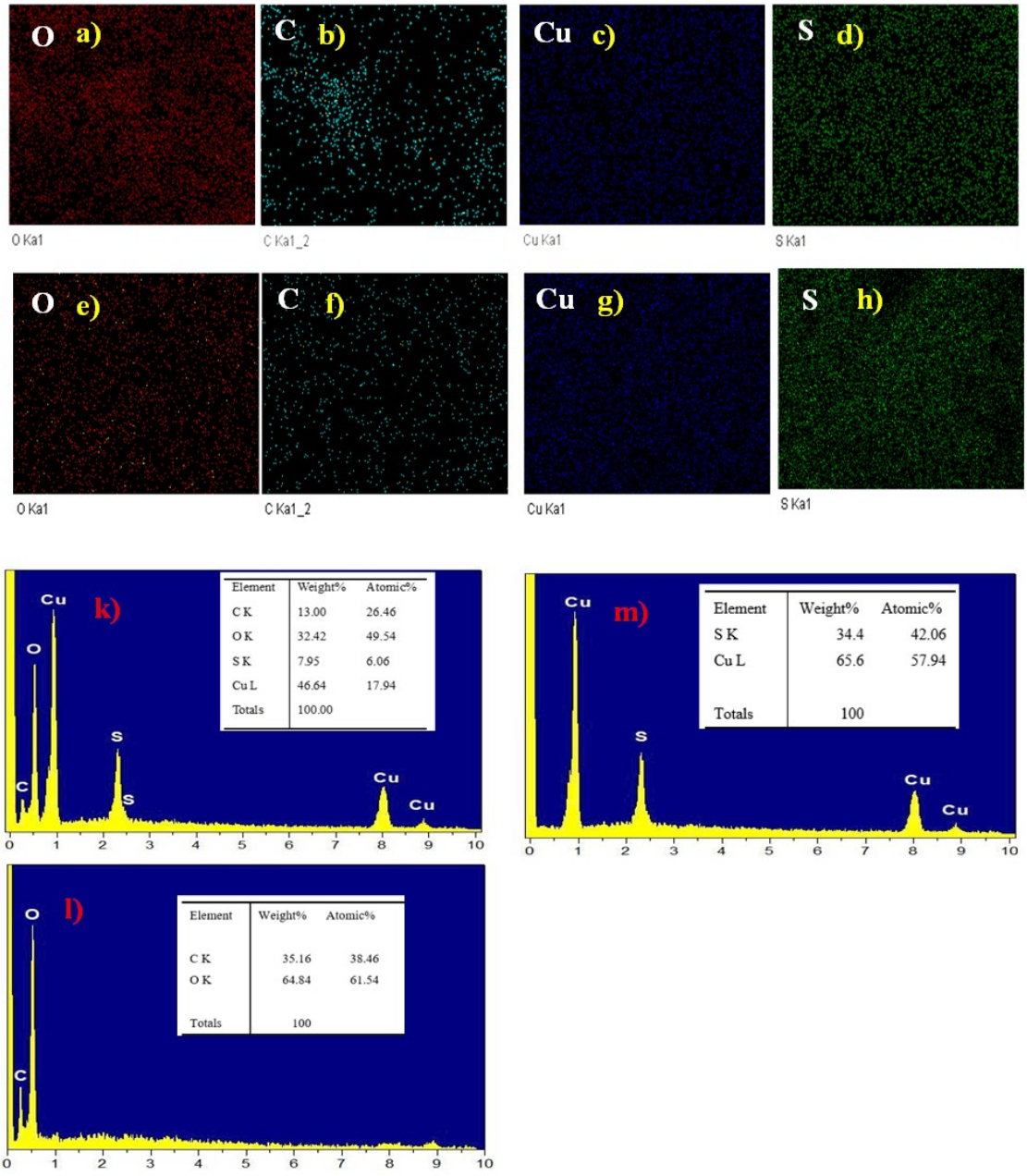

Figure 3. EDX Element Mapping Image of (A) Oxygen (O), (B) Carbon (C), (C) Copper (Cu) , (D) Sulphur (S), And (K) Atomic Percentage Of Elements Of Ergo@Cu_2S, E) Oxygen (O), F) Carbon (C) And (L) Atomic Percentage of Elements of Ergo, (G) Copper (Cu), (H) Sulphur (S), of (M) Atomic Percentage of Elements Of ECu_2S

well-dispersed and intimately contacted active phases, which are expected to facilitate charge transfer and enhance electrocatalytic activity at the counter electrode/electrolyte interface in QDSSCs.

The electrocatalytic behavior and charge-transfer dynamics of the prepared counter electrodes (CEs) were examined by cyclic voltammetry (CV) and electrochemical impedance spectroscopy (EIS) using a symmetric dummy cell filled with polysulfide electrolyte. Figure 4a shows the CV responses of ECu_2S, ErGO, and ErGO@Cu_2S within the potential range from -1.5 V to + 0.8 V versus Ag/AgCl. Among the tested electrodes, ErGO@Cu_2S delivered the most pronounced anodic and cathodic peaks, evidencing its superior catalytic activity toward the polysulfide redox couple (Sn^{2-}/S^{2-}). The ECu_2S electrode also displayed visible redox peaks, confirming its catalytic function, although its activity was constrained by lower electrical conductivity. By contrast, ErGO exhibited only small current densities and nearly featureless curves, suggesting that while

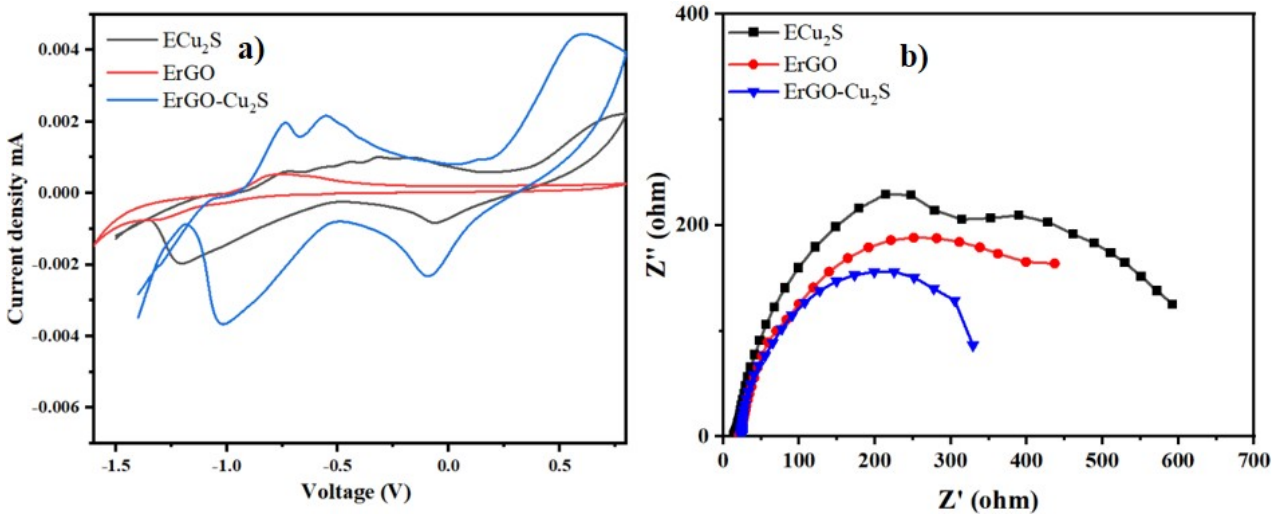

Figure 4. . a) CV Plots; b) Nyquist Plots (Inset: The Equivalent Circuit) of ErGO, ECu_2S, and ErGO@Cu_2S Films Electrode

it provides good conductivity, its direct catalytic contribution is limited. These observations underline the complementary roles of the two components: rGO establishes efficient charge-transport channels, while Cu_2S supplies abundant reaction sites for electrolyte regeneration.

Nyquist plots obtained from EIS measurements are provided in Figure 4b. Each spectrum shows a semicircle in the high-frequency domain, which corresponds to the charge-transfer resistance (Rct) at the CE/electrolyte interface. The hybrid ErGO@Cu_2S electrode produced the smallest semicircle, followed by ErGO and then ECu_2S, reflecting superior interfacial charge transport in the composite. The estimated Rct values were approximately 110 ω for ErGO@Cu_2S, 190 ω for ErGO, and 290 ω for ECu_2S. The substantially reduced resistance in the hybrid electrode indicates facilitated electron transfer and accelerated redox kinetics, consistent with the CV findings.

These results confirm that the electrodeposited ErGO@Cu_2S effectively integrates the advantages of both constituents, achieving lower interfacial resistance and higher catalytic efficiency. Notably, its performance rivals or surpasses that of other counter electrodes fabricated by more elaborate synthetic approaches. For instance, Prasad et al. (2021) obtained a PCE of 4.26% for a rGO-Cu_2S electrode produced by one-step co-electrodeposition followed by sulfurization, exceeding those of pristine Cu_2S (3.77%) and Pt (2.44%) (Krishna Prasad et al., 2021). Their improved efficiency was attributed to enhanced interfacial contact and reduced charge-transfer resistance enabled by the rGO scaffold. Similarly, Malavekar et al. (2020) reported rGO–CuS hybrids prepared through a combination of layer-by-layer assembly and the SILAR method, which exhibited high activity, large accessible surface area, and low resistance in supercapacitor devices-characteristics also desirable for solar cell CEs. Another study demonstrated that rGO-Cu_2S composites prepared via electrochemical reduction exhibited superior catalytic activity and durability due to strong interactions between Cu species and oxygenated graphene sheets. Compared with these strategies, our direct electrodeposition method provides a straightforward, low-temperature, and binder-free route that is scalable, while simultaneously ensuring competitive photovoltaic performance and excellent interfacial stability for QDSSCs.

Table 1. Photovoltaic J-V Characteristics of QDSSCs with ECu_2S, ErGO, and ErGO-Cu_2S Electrodes

Samples	J_{sc}/mA·cm^{-2}	Voc/V	FF/%	η/%
ErGO	15.2	0.44	40	3.24
ECu_2S	15.7	0.48	50	3.77
ErGO–Cu_2S	20.95	0.52	44	4.65

The photovoltaic performance of the quantum dot-sensitize d solar cells (QDSSCs) assembled with ErGO, ECu_2S, and ErGO-Cu_2S counter electrodes was evaluated under simulated AM 1.5G solar irradiation (100 mW.cm^{-2}), and the results are summarized in Figure 4 and Table 1. As shown in the J–V curves (Figure 5), the QDSSC employing the ErGO-Cu_2S counter electrode exhibited the highest short-circuit current density (Jsc) of 20.95 mA·cm^{-2}, an open-circuit voltage (Voc) of 0.52 V, and a fill factor (FF) of 44%, leading to a power conversion efficiency (PCE, η) of 4.65%. This performance surpasses that of the individual components, namely ErGO (η = 3.24%) and ECu_2S (η = 3.77%). The enhanced Jsc and Voc observed in the ErGO–Cu_2S-based device can be attributed to the synergistic effects between the excellent conductivity and large surface area of rGO and the high catalytic activity of Cu_2S. The rGO matrix provides efficient charge transport pathways, whereas Cu_2S facilitates rapid electron transfer and efficient redox reactions in the polysulfide electrolyte. The device using only ErGO as the CE exhibited the lowest Jsc (15.2

Table 2. Comparison of the Power Efficiency of QDSSCs Based on Different Fabricated rGO@Cu_2S CEs

CE Material	Method	J_{sc} (mA·cm^{-2})	V_{oc} (V)	FF	η (%)	Reference
rGO–CuS	Solvothermal	17.1	0.58	48	4.76	(Yuan et al., 2018)
$Cu_{1.81}S$–GOR	Microwave synthesis	18.04	0.52	58	3.55–6.81	(Ghosh et al., 2016)
rGO–Cu_2S	Co-electrodeposition + sulfurization	17.2	0.56	44	4.26	(Krishna Prasad et al., 2021)
NiSe	Electrodeposition (PVE)	16.53	0.53	51.3	4.46	(Lee et al., 2019)
CuInSe	Electrodeposition	16.53	0.53	51.3	2.92	(Guo et al., 2018)
ErGO–Cu_2S	Electrochemical deposition	20.95	0.52	44	4.65	This study

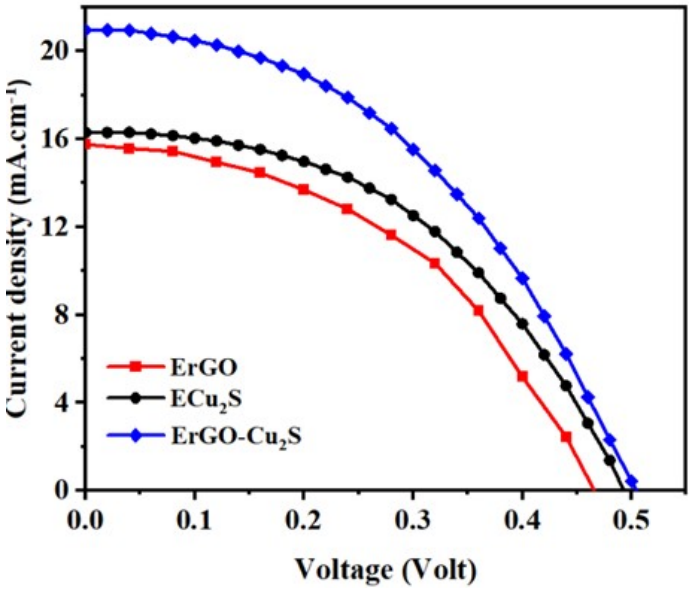

Figure 5. a) J-V Curves of QDSSC Base ErGO, ECu_2S, and ErGO@Cu_2S Counter Electrodes

mA·cm^{-2}) and Voc (0.44 V), which is consistent with its weak catalytic behavior, as observed in the CV and EIS analyses. The ECu_2S electrode offers improved Voc and FF owing to its catalytic nature, but it still suffers from higher charge-transfer resistance than the hybrid electrode. The superior photovoltaic performance of the ErGO-Cu_2S CE validates the advantages of the electrochemical co-deposition strategy, which enables intimate contact between the two phases and enhances interfacial electron transport. These results further confirm the findings from the electrochemical characterization and highlight that the rGO-Cu_2S hybrid CE prepared via a low-temperature and scalable electrodeposition route can serve as a viable alternative to noble-metal-based CEs in QDSSCs.

These findings suggest that the electrochemically deposited ErGO–Cu_2S composite effectively combines the advantages of both rGO and Cu_2S, leading to improved interfacial charge transfer and catalytic activities. The obtained power conversion efficiency (PCE) of 4.65% not only surpasses those of pure rGO (3.24%) and Cu_2S (3.77%) electrodes but also demonstrates the strong potential of this facile, low-temperature approach for practical applications in QDSSCs. This performance is comparable to, and in some cases superior to, the counter electrodes synthesized using more complex or thermally demanding methods, as shown in Table 2. For example, Yuan et al. (2018) prepared RGO/Cu_2S CEs via a solvothermal method, achieving a PCE of 4.76%, which was attributed to the enhanced conductivity and reduced charge transfer resistance at the CE/electrolyte interface. Ghosh et al. (2016) employed a microwave-assisted synthesis to fabricate $Cu_{1.1s}S$–graphene oxide nanoribbon composites, reporting a PCE of 3.55% for CdS-sensitized and up to 6.81% for CdTe/CdS co-sensitized QDSSCs, citing the quasi-one-dimensional structure of GOR for improved catalytic edge density and stability. Malavekar et al. (2020) developed rGO–CuS hybrid electrodes using the SILAR + LBL method for supercapacitor applications, highlighting the structural synergy and ion diffusion advantages offered by the layered design. In contrast, our one-step electrochemical deposition strategy offers several distinct advantages: it eliminates the need for high-temperature treatments, surfactants, or multi-step processes; it enables direct growth on conductive substrates with strong film adhesion; and it remains highly scalable for industrial use. Furthermore, our method produced a hybrid film with a competitive photovoltaic output and excellent electrocatalytic behavior, as supported by the CV, EIS, and J-V results. These benefits collectively position electrochemically deposited ErGO-Cu_2S as a practical and efficient counter electrode material for next-generation QDSSCs.

4. CONCLUSIONS

In this study, we successfully fabricated rGO, Cu_2S, and rGO@Cu_2S counter electrodes via a facile and low-temperature electrochemical deposition method for application in quantum-dot-sensitized solar cells (QDSSCs). The individual components exhibited complementary properties: Cu_2S offered high catalytic activity toward the polysulfide redox couple, and rGO provided excellent electrical conductivity and structural stability. The hybrid rGO-Cu_2S electrode effectively integrated these advan-

tages, resulting in enhanced charge transport and improved redox kinetics. Electrochemical characterizations, including cyclic voltammetry (CV) and electrochemical impedance spectroscopy (EIS), confirmed the superior electrocatalytic performance and reduced charge transfer resistance of the rGO-Cu_2S composite compared to those of the individual materials. Correspondingly, the QDSSC employing the rGO-Cu_2S CEs achieved the highest PEC of 4.65%, outperforming those with Cu_2S (3.77%) and rGO (3.24%) counter electrodes. These results demonstrate that electrochemical deposition is an effective strategy for fabricating high-performance, low-cost, and scalable hybrid counter electrodes for DSSCs. The synergistic enhancement observed in the rGO-Cu_2S system provides valuable insights for the future development of alternative CEs in QDSSCs and other photoelectrochemical devices.

5. ACKNOWLEDGMENT

This research is supported by the Industrial University of Ho Chi Minh City (IUH).

REFERENCES

Chung, N. T. K., P. T. Nguyen, H. T. Tung, and D. H. Phuc (2021). Quantum Dot Sensitized Solar Cell: Photoanodes, Counter Electrodes, and Electrolytes. *Molecules*, **26**(9); 2638

Dang, H. P., H. T. Tung, N. T. M. Hanh, N. T. K. Duyen, V. T. N. Thuy, N. T. H. Anh, and L. V. Hieu (2024). Efficient Counter Electrode for Quantum Dot Sensitized Solar Cells Using P-Type PbS@Reduced Graphene Oxide Composite. *Nanoscale Advances*, **7**(3); 700–710

Du, Z., Z. Pan, F. Fabregat-Santiago, K. Zhao, D. Long, H. Zhang, and J. Bisquert (2016). Carbon Counter-Electrode-Based Quantum-Dot-Sensitized Solar Cells with Certified Efficiency Exceeding 11%. *Journal of Physical Chemistry Letters*, **7**(16); 3103–3111

Eryiğit, M., S. Mobtakeri, E. P. Gür, E. Temur, T. O. Özer, U. Demir, and E. Gür (2022). Efficient CdS Quantum Dot Sensitized Solar Cells Based on Electrochemically Reduced Graphene Oxide (ERGO)/ZnO Nanowall Photoanodes and MoS_2, WS_2, CuS Cascaded Counter Electrodes. *Solar Energy*, **234**; 348–359

Ghosh, D., G. Halder, A. Sahasrabudhe, and S. Bhattacharyya (2016). A Microwave Synthesized CuxS and Graphene Oxide Nanoribbon Composite as a Highly Efficient Counter Electrode for Quantum Dot Sensitized Solar Cells. *Nanoscale*, **8**(20); 10632–10641

Guo, H., R. Zhou, Y. Huang, L. Wan, W. Gan, H. Niu, and J. Xu (2018). Electrodeposited $CuInSe_2$ Counter Electrodes for Efficient and Stable Quantum Dot-Sensitized Solar Cells. *Ceramics International*, **44**(13); 16092–16098

Jo, I. R., J. A. Rajesh, Y. H. Lee, J. H. Park, and K. S. Ahn (2020). Enhanced Electrocatalytic Activity and Electrochemical Stability of Cu_2S/PbS Counter Electrode for Quantum-Dot-Sensitized Solar Cells. *Applied Surface Science*, **525**; 146643

Krishna Prasad, A., I. R. Jo, S. H. Kang, and K. S. Ahn (2021). Novel Method for Synthesis of Reduced Graphene Oxide–Cu_2S and Its Application as a Counter Electrode in Quantum-Dot-Sensitized Solar Cells. *Applied Surface Science*, **564**; 150393

Kusumawati, N., P. Setiarso, S. Muslim, Q. A. Hafidha, S. A. Cahyani, and F. F. Fachrirakarsie (2024). Optimization Thickness of Photoanode Layer and Membrane as Electrolyte Trapping Medium for Improvement Dye-Sensitized Solar Cell Performance. *Science and Technology Indonesia*, **9**(1); 7–16

Lee, Y.-H., Y.-H. Yun, V. Hong Vinh Quy, S.-H. Kang, H. Kim, E. Vijayakumar, and K.-S. Ahn (2019). Preparation of Nickel Selenide by Pulsed-Voltage Electrodeposition and Its Application as a Highly-Efficient Electrocatalyst at Counter Electrodes of Quantum-Dot Sensitized Solar Cells. *Electrochimica Acta*, **296**; 364–371

Li, W., S. Zhang, Q. Chen, and Q. Zhong (2022). Highly-Dispersed CoS_2/N-Doped Carbon Nanoparticles Anchored on RGO Skeleton as a Hierarchical Composite Counter Electrode for Quantum Dot Sensitized Solar Cells. *Chemical Engineering Journal*, **430**; 132732

López-Rojas, O., M. del Socorro Aguilar, J. de Jesús Ku-Herrera, R. M. Jiménez-Barrera, V. H. López, J. García, and T. López-Luke (2024). Photoelectrochemical Study of the Performance Enhancement of CNT-Based Counter Electrodes by Adding N-S Doped rGO in QD Solar Cells: Photoelectrochemical Study of the Performance Enhancement of CNT-Based Counter Electrodes. *Journal of Electronic Materials*, **54**(2); 1141–115

Malavekar, D. B., V. C. Lokhande, V. J. Mane, S. B. Kale, R. N. Bulakhe, U. M. Patil, and C. D. Lokhande (2020). Facile Synthesis of Layered Reduced Graphene Oxide–Copper Sulfide (rGO–CuS) Hybrid Electrode for All Solid-State Symmetric Supercapacitor. *Journal of Solid State Electrochemistry*, **24**(11–12); 2963–2974

Mehmood, U. and A. Ul Haq Khan (2019). Spray Coated PbS Nano-Crystals as an Effective Counter-Electrode Material for Platinum Free Dye-Sensitized Solar Cells (DSSCs). *Solar Energy*, **193**; 1–5

Meng, K., G. Chen, and K. R. Thampi (2015). Metal Chalcogenides as Counter Electrode Materials in Quantum Dot Sensitized Solar Cells: A Perspective. *Journal of Materials Chemistry A*, **3**; 23074–23089

Monika, S., M. Mahalakshmi, N. Subha, M. S. Pandian, and P. Ramasamy (2022). Graphene Quantum Dots and CuS Microflowers Anchored rGO Composite Counter Electrode for the Enhanced Performance of Quantum Dot Sensitized Solar Cells. *Diamond and Related Materials*, **125**; 109033

My Hanh, N. T., H. T. Tung, N. T. K. Duyen, V. C. Nguyen, L. Van Hieu, N. T. Nguyen, and H. P. Dang (2024). Effect of Hydrothermal Time on Catalyst Activity of Counter Electrode Cu_2S–rGO Composite to Enhance the Efficiency of Quantum Dot Solar Cells. *Ceramics International*, **50**(15); 27127–27138

Nozik, A. J. (2002). Quantum Dot Solar Cells. *Physica E: Low-Dimensional Systems and Nanostructures*, **14**(1–2); 115–120

Prasad, A. K., I.-R. Jo, S.-H. Kang, and K.-S. Ahn (2021). Novel Method for Synthesis of Reduced Graphene Oxide–Cu_2S and Its Application As a Counter Electrode in Quantum-Dot-Sensitized Solar Cells. *Applied Surface Science*, **564**; 150393

Que, M., W. Guo, X. Zhang, X. Li, Q. Hua, L. Dong, and C. Pan (2014). Flexible Quantum Dot-Sensitized Solar Cells Employing CoS Nanorod Arrays/Graphite Paper as Effective Counter Electrodes. *Journal of Materials Chemistry A*, **2**(33); 13661–13667

Radich, E. J., R. Dwyer, and P. V. Kamat (2011). Cu_2S Reduced Graphene Oxide Composite for High-Efficiency Quantum Dot Solar Cells: Overcoming the Redox Limitations of S_2^-/Sn_2^- at the Counter Electrode. *Journal of Physical Chemistry Letters*, **2**(19); 2453–2460

Rathnavel, P., C. Murukesh, and R. Umamaheswari (2023). Fabrication of a Novel rGO Encapsulated Nickel Cobalt Chalcogenide Electrocatalyst as an Efficient Counter Electrode to Boost Efficiency of Dye-Sensitized Solar Cells. *Journal of Materials Science: Materials in Electronics*, **34**(11); 8159–8170

Telussa, I., E. G. Fransina, E. R. M. A. P. Lilipaly, and A. M. I. Efruan (2022). Effect of Photosynthetic Pigment Composition of Tropical Marine Microalgae from Ambon Bay Navicula sp. TAD on Dye-Sensitized Solar Cell Efficiency. *Science and Technology Indonesia*, **7**(4); 486–491

Tian, Z., Q. Chen, and Q. Zhong (2020). Honeycomb Spherical 1T-MoS_2 as Efficient Counter Electrodes for Quantum Dot Sensitized Solar Cells. *Chemical Engineering Journal*, **396**; 125374

Van Le, N., H. T. Nguyen, H. V. Le, and T. T. P. Nguyen (2017). Lead Sulfide Cathode for Quantum Dot Solar Cells: Electrosynthesis and Characterization. *Journal of Electronic Materials*, **46**(1); 274–281

Van Thang, B., H. T. Tung, D. H. Phuc, T. P. Nguyen, T. Van Man, and L. Q. Vinh (2023). High-Efficiency Quantum Dot Sensitized Solar Cells Based on Flexible rGO-Cu_2S Electrodes Compared with PbS, CuS, Cu_2S CEs. *Solar Energy Materials and Solar Cells*, **250**; 112042

Wang, J., M. M. Rahman, C. Ge, and J.-J. Lee (2018). Electrodeposition of Cu_2S Nanoparticles on Fluorine-Doped Tin Oxide for Efficient Counter Electrode of Quantum-Dot-Sensitized Solar Cells. *Journal of Industrial and Engineering Chemistry*, **62**; 185–191

Yang, W., Y. Sun, P. Yang, and X. Chen (2019). CoS/Nanocarbon Composite as a Catalytic Counter Electrode for Improved Performance of Quantum Dot-Sensitized Solar Cells. *Journal of Nanomaterials*, **2019**; 2710712

Ye, M., C. Chen, N. Zhang, X. Wen, W. Guo, and C. Lin (2014). Quantum-Dot Sensitized Solar Cells Employing Hierarchical Cu_2S Microspheres Wrapped by Reduced Graphene Oxide Nanosheets as Effective Counter Electrodes. *Advanced Energy Materials*, **4**(9); 1301564

Yuan, B., Q. Gao, X. Zhang, L. Duan, L. Chen, Z. Mao, and W. Lü (2018). Reduced Graphene Oxide (RGO)/Cu_2S Composite as Catalytic Counter Electrode for Quantum Dot-Sensitized Solar Cells. *Electrochimica Acta*, **277**; 50–58

Zhang, X., L. Duan, X. Zhang, X. Li, and W. Lü (2020). Preparation of Cu_2S@rGO Hybrid Composites as Anode Materials for Enhanced Electrochemical Properties of Lithium Ion Battery. *Journal of Alloys and Compounds*, **816**; 152539

